International Journal of Applied Mathematics and Computation
Volume 2(1),pp 11–31, 2010
http://ijamc.psit.in

Trajectory Planning and Posture Control of Multiple Mobile Manipulators

Bibhya N. Sharma[1], Jito Vanualailai[2] and Avinesh Prasad[3]

School of Computing, Information & Mathematical Sciences
University of the South Pacific, Suva, FIJI
E-mail: [1]*sharma-b@usp.ac.fj,* [2]*vanualailai@usp.ac.fj,* [3]*prasad-ai@usp.ac.fj*

Abstract:

We propose an algorithm as a solution to the problem of trajectory planning and posture control of multiple mobile manipulators within a fixed and bounded but obstacle-ridden workspace. This, together with other kinematic and dynamics constraints normally integrated to the mobile manipulators have been treated simultaneously, for the first time, via a Lyapunov-based control scheme. The control scheme guarantees stability of the system, per se. We have accounted for the final orientations of the wheeled platforms and the attached links using a new optimization technique classified as *minimum distance technique* (MDT). The technique coupled with tuning parameters force prescribed orientations of the mobile manipulators. Efficiency of the new control algorithm is demonstrated via a couple of interesting computer simulations.

Keywords: Mobile manipulators, kinematic constraints, dynamic constraints, posture, Lyapunov-based control scheme, minimum distance technique, stability analysis.

1 Introduction

Trajectory planning and control of holonomic and nonholonomic systems has been an active area of research and has garnered monumental support and attention for more than two decades now. The literature is inundated with algorithms, strategies and schemes governing motion control of various robotic systems. The reasons for this is multifold: strong presence of mechanical systems that have non-integrable constraints such as robot manipulators, mobile robots, wheeled vehicles, and space and underwater robots; its wide-ranging capabilities; considerable challenge in the synthesis of control laws for systems that are not transferable into linear control problems in any meaningful way; and as a direct result of Brockett's theorem [1] the failure to procure stabilizing feedback control laws of nonholonomic systems.

Corresponding author: **Bibhya N. Sharma**

The control algorithms and strategies have been categorized into three groups, namely continuous time-variant, discontinuous and hybrid control strategies [9, 21]. Numerous continuous time-invariant feedback control laws have appeared in literature [22, 23] which have guaranteed stability of robotic systems, per se. However, to show asymptotic stability with smooth controllers, in light of Brockett's theorem, is still an open problem.

One of the challenging problems in the area of motion planning and control of robots is to generate specific configurations in constraint environments. Studies [7, 11, 23, 24] have considered the motion planning problem of robot arms anchored in constraint environments. Meyer in [11] pioneered a findpath scheme based on velocities of the various components of anchored robot arms. Vanualailai et. al. in [23, 24] extended Meyer's work by applying the Lyapunov-based control scheme to generate continuous control laws based upon the acceleration components of anchored robots. In the prequel [18], we extended the work further by applying the control scheme to an unanchored 2-link manipulator.

Of the many mechanical systems in literature, the mobile manipulators play a pivotal role in the transportation industry nowadays and are capable of performing dull, dirty, dangerous or difficult tasks in various different environments, which may be even inaccessible to humans [5]. The pioneer work with the mobile manipulators was carried out by Seraji [14], which is now considered a landmark in the literature of motion control of the mobile manipulators. Other researchers have proposed efficient algorithms for the control of the mobile manipulators and it suffices to mention a few important ones: Perriera et al. [13], Huang et al. [6] and Foulon et al. [2, 3] in 1998; Foulon et al. [4] in 1999; Papadopoulos and Poulakakis [12] in 2000; Sugar and Kumar [20] in 2002; Matsikis et al. [10] in 2003; and Xu et al. [25] in 2005. In this ever-growing repertoire, the 2-link mobile manipulators are deemed to be more difficult to control, the arterial reason being the intimate coupling of holonomic and nonholonomic constraints arising from the amalgamation of a 2-link robotic arm and a wheeled platform. As such the task of motion planning and control of 2-link mobile manipulators traversing the path to desired goals under a heavy barricade of obstacles is still a complicated one.

In this paper, we will extend the results in [18] to multiple unanchored 2-link manipulators, utilizing again the the Lyapunov-based control scheme to derive the feedback controllers. This control scheme adopted recently in [16, 19, 18, 17, 24] provides a simple but effective means of harnessing continuous time-invariant control laws of nonlinear dynamical systems. The control scheme operates within the artificial potential framework, which was pioneered by Khatib [8]. The governing principle behind the framework is to attach attractive field to the target and a repulsive field to each of the obstacles. The framework also offers an extended degree of flexibility by taking into account all the constraints pertaining the amalgamated robotic system which includes, inter alia, limitations on velocity and steering angle, singular configurations of the arms, restrictions imposed by boundary conditions, obstacles in workspace and point and posture stabilities. In parallel, the scheme addresses stability issues of the systems via Lyapunov's Second Method.

2 System Modelling

In this section, we derive the kinodynamic model of 2-link mobile manipulators using the Cartesian coordinates.

Let $A_i, i \in \{1, \ldots, n\}$ be the ith 2-link mobile manipulator included in the workspace WS. A_i consists of a car-like wheeled platform with a 2-link planar arm mounted on the mid-front axle of the wheeled platform as shown in Figure 1. For simplicity, we let each A_i to be of the same dimension; hence, ℓ_0 and b_0 are, respectively, the length and the width of the wheeled platforms while ℓ_1 and ℓ_2 are the length of their Link 1 and Link 2, respectively.

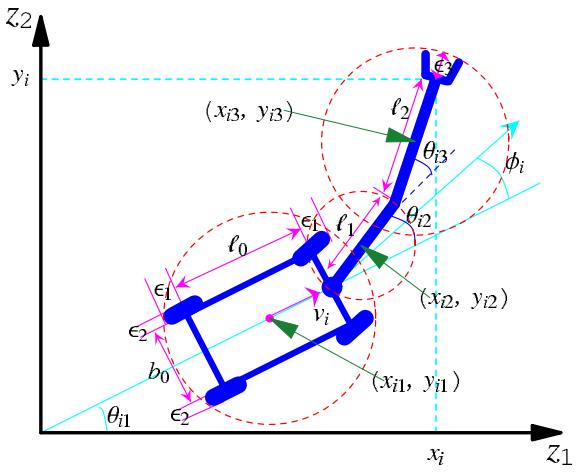

Figure 1: Schematic representation of the ith 2-link mobile manipulator in the z_1-z_2 plane.

With reference to Figure 1, (x_{i1}, y_{i1}) gives the location of the center of the wheeled platform of the ith mobile manipulator, θ_{i1} gives its orientation with respect to the z_1-axis, θ_{i2} gives the orientation of Link 1 with respect to its platform, θ_{i3} gives the orientation of Link 2 with respect to Link 1, while ϕ_i is the steering angle with respect to the platform's longitudinal axis.

We note the presence of the *clearance parameters* $\epsilon_1, \epsilon_2, \epsilon_3 > 0$ for safety of the wheeled platform and the gripper [18].

For the purpose of clarity, we shall now consider the governing equations of the wheeled platform and the 2-link arm separately and then combine them to obtain the governing ODE's of the ith 2-link mobile manipulator.

2.1 Car-like Wheeled Platform

Motion planning has been treated mostly as a kinematic problem where the dynamics of the system have been generally neglected. However, with nonholonomic systems, ignoring the dynamics reduces the significance of the results to low speeds although it is well documented that avoidance of obstacles, parking maneuverability, and mere motion control is feasible at higher speeds as well. Adopting the nomenclature of [16] the kinodynamic model of the ith car-like wheeled platform with respect to its center of mass (CoM) is governed via the ODEs:

$$\begin{aligned}
\dot{x}_{i1} &= v_i \cos\theta_{i1} - \frac{\ell_0}{2}\omega_{i1}\sin\theta_{i1}, \\
\dot{y}_{i1} &= v_i \sin\theta_{i1} + \frac{\ell_0}{2}\omega_{i1}\cos\theta_{i1}, \\
\dot{\theta}_{i1} &= \omega_{i1}, \quad \dot{v}_i = u_{i1}, \quad \dot{\omega}_{i1} = u_{i2},
\end{aligned}$$

where v_i and ω_{i1} are the translational and rotational velocities of the platform while u_{i1} and u_{i2} are its instantaneous translational and rotational accelerations, respectively.

2.2 2-link Manipulator

From the dossier on robot manipulators, we choose a fully actuated 2-link arm for the purpose of this research. Assume the link at the lower end is anchored at $(0, 0)$, the origin of the main frame, we adopt the following kinematic model of the 2-link arm from [24]:

$$\begin{aligned}
&\dot{x}_{ie} = -\ell_1\omega_{i2}\sin\theta_2 - \ell_2(\omega_{i2}+\omega_{i3})\sin(\theta_{i2}+\theta_{i3}),\\
&\dot{y}_{ie} = \ell_1\omega_{i2}\cos\theta_{i2} + \ell_2(\omega_{i2}+\omega_{i3})\cos(\theta_{i2}+\theta_{i3}),\\
&\dot{\theta}_{i2} = \omega_{i2}, \quad \dot{\theta}_{i3} = \omega_{i3},\\
&\dot{\omega}_{i2} = u_{i3}, \quad \dot{\omega}_{i3} = u_{i4},
\end{aligned}$$

where ω_{i2} and ω_{i3} are the instantaneous angular velocities, and u_{i3} and u_{i4} are the instantaneous angular accelerations, respectively, of the lower and upper links of the robot arm.

2.3 2-link Mobile Manipulator

Let us now consider the wheeled platform and the 2-link arm fixed together as one complete robot unit, hereafter, classified as a 2-link mobile manipulator (2MM). The position (x_i, y_i) of its end-effector with respect to its wheeled platform can be written as :

$$\begin{aligned}
x_i &= x_{i1} + \frac{\ell_0}{2}\cos\theta_{i1} + \ell_1\cos(\theta_{i1}+\theta_{i2}) + \ell_2\cos(\theta_{i1}+\theta_{i2}+\theta_{i3}),\\
y_i &= y_{i1} + \frac{\ell_0}{2}\sin\theta_{i1} + \ell_1\sin(\theta_{i1}+\theta_{i2}) + \ell_2\sin(\theta_{i1}+\theta_{i2}+\theta_{i3}).
\end{aligned}$$

Now letting $\theta_{iQ} = \theta_{i1}+\theta_{i2}$, $\theta_{iT} = \theta_{i1}+\theta_{i2}+\theta_{i3}$, $\omega_{iQ} = \omega_{i1}+\omega_{i2}$ and $\omega_{iT} = \omega_{i1}+\omega_{i2}+\omega_{i3}$ one can comfortably show that the kinodynamic model of the ith 2MM is

$$\left.\begin{aligned}
&\dot{x}_i = v_i\cos\theta_{i1} - \ell_0\omega_{i1}\sin\theta_{i1} - \ell_1\omega_{iQ}\sin\theta_{iQ} - \ell_2\omega_{iT}\sin\theta_{iT},\\
&\dot{y}_i = v_i\sin\theta_{i1} + \ell_0\omega_{i1}\cos\theta_{i1} + \ell_1\omega_{iQ}\cos\theta_{iQ} + \ell_2\omega_{iT}\cos\theta_{iT},\\
&\dot{\theta}_{i1} = \omega_{i1}, \qquad \dot{\theta}_{i2} = \omega_{i2}, \qquad \dot{\theta}_{i3} = \omega_{i3},\\
&\dot{v}_i = u_{i1}, \qquad \dot{\omega}_{i1} = u_{i2}, \qquad \dot{\omega}_{i2} = u_{i3}, \qquad \dot{\omega}_{i3} = u_{i4}.
\end{aligned}\right\} \tag{2.1}$$

System (2.1) is a description of the instantaneous velocities and accelerations of the various bodies of A_i. We assume that the instantaneous accelerations u_{i1}, u_{i2}, u_{i3} and u_{i4} can move the end-effector of A_i to its designated target and will ensure the final orientation prescribed to each rigid body inside the parking bay. Hence, by the Lyapunov-based control scheme, $(u_{i1}, u_{i2}, u_{i3}, u_{i4})$ for $i = 1, 2, \ldots, n$ are considered as the nonlinear controllers of the 2MMs.

We shall use the vector notation $\mathbf{x}_i = (x_i, y_i, \theta_{i1}, \theta_{i2}, \theta_{i3}, v_i, \omega_{i1}, \omega_{i2}, \omega_{i3}) \in \mathbb{R}^9$ in the z_1-z_2 plane to refer to the position and velocity components of A_i. Without any loss of generality, we can further define $\mathbf{x} = (\mathbf{x}_1, \mathbf{x}_2, \ldots, \mathbf{x}_n) \in \mathbb{R}^{9\times n}$ to include the position and velocity components of all 2MMs populating the workspace.

It is easily verifiable that the positions of the wheeled platform, Link 1 and Link 2 of the ith 2MM can be expressed completely in terms of the state variables x_i, y_i, θ_{i1}, θ_{i2}, and θ_{i3}, hence for the articulated bodies $m = 1, 2, 3$ of A_i we ascertain

$$\left.\begin{aligned} x_{im} &= x_i - \sum_{k=m}^{3} \frac{\ell_{k-1}}{2^{\lfloor m/k \rfloor}} \cos\left(\sum_{p=1}^{k} \theta_{ip}\right), \\ y_{im} &= y_i - \sum_{k=m}^{3} \frac{\ell_{k-1}}{2^{\lfloor m/k \rfloor}} \sin\left(\sum_{p=1}^{k} \theta_{ip}\right). \end{aligned}\right\} \tag{2.2}$$

These position constraints are known as the *holonomic constraints* of the 2-link mobile manipulator system.

3 Motion Planning

In this section, we will plan collision free motions of n 2MMs in a constrained and well-defined workspace. But to ensure that each 2MM safely steers past an obstacle, it is necessary to enclose each rigid body of the 2MM by the smallest possible circle. Given the clearance parameters we shall enclose the wheeled platform by a protective circular region centered at (x_{i1}, y_{i1}) with radius $r_1 = \frac{1}{2}\sqrt{(\ell_0 + 2\epsilon_1)^2 + (b_0 + 2\epsilon_2)^2}$. Similarly, we shall enclose Link 1 and Link 2 in protective circular regions of radii $r_2 = \frac{\ell_1}{2}$ and $r_3 = \frac{\ell_2}{2} + \epsilon_3$, respectively, and denote their centers as (x_{i2}, y_{i2}) and (x_{i3}, y_{i3}), respectively (as shown in Figure 1). This is in line with the work carried out in [18].

***Control objective*:** Utilize the Lyapunov-based control scheme to control the motion of $A_i, i \in \{1, \ldots, n\}$ to the designated target while ensuring that it avoids all fixed and moving obstacles in the constrained workspace and eventually reach its target inside the designated parking bay with a prescribed final orientation of each solid body.

We define below the targets and all the obstacles that could be encountered by A_i. For each different subtask, appropriate artificial potential fields would be produced separately to help achieve the overall objective. On one hand, we design a *target attractive function* for attraction to a target. This function can be treated as an attractive potential field function. On the other hand, we have the *obstacle avoidance function* designed to avoid an obstacle encountered in the workspace. Repulsive potential field functions would then be designed from such avoidance functions. Each avoidance function would appear in the denominator of a potential field function while the numerator would contain a unique tuning parameter. These potential field functions would be summed into a Lyapunov function from which the nonlinear controllers would be generated. The reader is referred to [15] for further details on the Lyapunov-based control scheme.

3.1 Posture

In this section we shall consider the position and the orientation modules of posture separately to highlight and elucidate the importance of our new technique. We also make the following assumption:

Assumption: The prescribed final posture (position and orientation) is required inside a parking bay prescribed to the 2MM.

3.1.1 Position

We need to affix a target for each robot to reach after some time $t > 0$. Hence we designate a target for the end-effector of A_i with center (p_{i1}, p_{i2}) and radius rt_i: $T_i = \{(z_1, z_2) \in \mathbb{R}^2 : (z_1 - p_{i1})^2 + (z_2 - p_{i2})^2 \leq rt_i^2\}$. For its attraction we consider the following target attractive function

$$H_i(\mathbf{x}) = \frac{1}{2}\left[(x_i - p_{i1})^2 + (y_i + p_{i2})^2 + \sum_{j=2}^{3} \rho_{ij}(\theta_{ij} - p_{ij+2})^2 + v_i^2 + \sum_{k=1}^{3} \omega_{ik}^2\right], \qquad (3.1)$$

which is positive for all $\mathbf{x} \in \mathbb{R}^{9\times n}$. Note that $\rho_{i2}, \rho_{i3} > 0$ are the newly inducted constants, classified as the *angle-gain parameters*. An angle-gain parameter will have a value of one only if a final orientation is warranted, else it observes a default value of zero [15]. In the Lyapunov-based control scheme, once a Lyapunov function for system (2.1) is established $H_i(\mathbf{x})$ will act as attractor by having the end-effector of A_i move to its target and to ensure that system trajectories start and remain close to a stable equilibrium point of system (2.1).

3.1.2 Orientation

Although the final position is reachable, it is virtually impossible to harvest exact orientations via continuous feedback controllers at the equilibrium point of nonholonomic systems, a direct result of Brockett's Theorem [1]. Notwithstanding the limitation, we adopt the *minimum distance technique* (MDT) from [15] to maneuver each 2MM into a parking bay such that the prescribed final orientation could also be accomplished, at least numerically. In the interest of brevity, we will now consider the processes involved in MDT.

Basically, a boundary line of a parking bay is avoided by identifying and avoiding three points on the line: (i) point closest to the center of the mobile platform, (ii) point closest to the center of Link 1, and (iii) point closest to the center of Link 2. Avoidance of these points on a line segment at any time $t \geq 0$ essentially results in the avoidance of the entire boundary line by the complete 2MM. MDT specifically requires consideration of any kth line segment in the z_1z_2-plane with initial coordinates (a_{k1}, b_{k1}) and final coordinate (a_{k2}, b_{k2}). The parametric representation of this kth line segment is

$$c_{imk} = a_{k1} + \lambda_{imk}(a_{k2} - a_{k1}), \quad d_{imk} = b_{k1} + \lambda_{imk}(b_{k2} - b_{k1})\ .$$

where $m = 1, 2, 3$ are the three solid bodies of A_i. Minimizing the Euclidian distance between the point (x_{im}, y_{im}) and the line segment (c_{imk}, d_{imk}), we get

$$\lambda_{imk} = (x_{im} - a_{k1})q_{k1} + (y_{im} - b_{k1})q_{k2}, \text{ for } \lambda_{imk} \in [0, 1]\ ,$$

where

$$q_{k1} = \frac{(a_{k2} - a_{k1})}{(a_{k2} - a_{k1})^2 + (b_{k2} - b_{k1})^2}, \qquad q_{k2} = \frac{(b_{k2} - b_{k1})}{(a_{k2} - a_{k1})^2 + (b_{k2} - b_{k1})^2}.$$

The following obstacle avoidance function will ensure that each of the m bodies of A_i will avoid the closest point on the kth boundary line of a parking bay

$$LS_{imk}(\mathbf{x}) \;=\; \frac{1}{2}\left[(x_{im}-c_{imk})^2+(y_{im}-d_{imk})^2-r_m^2\right], \tag{3.2}$$

for $m = 1, 2, 3$, $k = 1, 2, \ldots, 2n$ and $i = 1, 2, \ldots, n$. As discussed previously, to generate repulsive effects from this function we design a new repulsive potential field function which is basically an inverse function that encodes the avoidance function to the denominator. This ratio acts to prevent the articulated vehicle from colliding with the boundary lines. The main idea here is to attach necessary and sufficient repulsive fields to the boundary lines of the parking bay so that the prescribed final orientations could be *forced* to eventuate [15].

Henceforth, for each obstacle, we will construct an obstacle avoidance function that will then appear in the denominator of an appropriate repulsive potential field function.

3.2 Kinematic Constraints

The kinematic constraints are the nonholonomy of the 2MMs and all the fixed and moving obstacles in the workspace. The nonholonomy of the robot is reflected in the kinodynamic model (2.1). The fixed obstacles are the four boundaries of the rectangular workspace, all stationary obstacles in the workspace and the boundaries of the parking bays. The moving obstacles in this research are the mobile manipulators themselves.

3.2.1 Workspace: Boundary Limitations

We adopt the planar workspace from [16], which is a fixed, closed, and bounded rectangular region defined for $\eta_1 > 2\,(r_1 + r_2 + r_3)$ and $\eta_2 > 2\,(r_1 + r_2 + r_3)$, as

$$WS = \{(z_1, z_2) \in \mathbb{R}^2 : 0 \le z_1 \le \eta_1, 0 \le z_2 \le \eta_2\}.$$

The boundaries of the region are defined as follows:

(a) Left Boundary: $B_1 = \{(z_1, z_2) \in \mathbb{R}^2 : z_1 = 0\}$;

(b) Lower Boundary: $B_2 = \{(z_1, z_2) \in \mathbb{R}^2 : z_2 = 0\}$;

(c) Right Boundary: $B_3 = \{(z_1, z_2) \in \mathbb{R}^2 : z_1 = \eta_1\}$;

(d) Upper Boundary: $B_4 = \{(z_1, z_2) \in \mathbb{R}^2 : z_2 = \eta_2\}$.

These boundaries are considered as *fixed obstacles*, and they have to be avoided by the 2MMs so that they stay within the rectangular region at all time $t \ge 0$. It can be seen that since the two ends of Link 1 are protected by the protective circular regions of the wheeled platform and of Link 2, respectively, it is sufficient to consider the avoidance functions only for the wheeled platform and Link 2 of A_i.

As such, for the avoidance by the wheeled platform we shall adopt the following obstacle avoidance functions [16]:

$$W_{i1}(\mathbf{x}) := x_{i1} - r_1\,, \qquad W_{i2}(\mathbf{x}) := y_{i1} - r_1, \tag{3.3a-b}$$

$$W_{i3}(\mathbf{x}) := \eta_1 - (r_1 + x_{i1}), \qquad W_{i4}(\mathbf{x}) := \eta_2 - (r_1 + y_{i1}), \tag{3.3c-d}$$

while for Link 2, we have:

$$W_{i5}(\mathbf{x}) := x_{i3} - r_3\ , \qquad W_{i6}(\mathbf{x}) := y_{i3} - r_3, \tag{3.4a-b}$$

$$W_{i7}(\mathbf{x}) := \eta_1 - (r_3 + x_{i3}), \qquad W_{i8}(\mathbf{x}) := \eta_2 - (r_3 + y_{i3}), \tag{3.4c-d}$$

for the avoidance of the left, lower, right and upper boundaries, respectively. Since $\eta_1 > 2\,(r_1 + r_2 + r_3)$ and $\eta_2 > 2\,(r_1 + r_2 + r_3)$, each of the aforementioned functions is positive in WS. That is, $W_{i1}, W_{i3} > 0$ for all $x_{i1} \in (r_1, \eta_1 - r_1)$, $W_{i2}, W_{i4} > 0$ for all $y_{i1} \in (r_1, \eta_2 - r_1)$, $W_{i5}, W_{i7} > 0$ for all $x_{i3} \in (r_3, \eta_1 - r_3)$, and $W_{i6}, W_{i8} > 0$ for all $y_{i3} \in (r_3, \eta_2 - r_3)$, for $i = 1, 2, \ldots, n$, recalling that the forms of (x_{i1}, y_{i1}) and (x_{i3}, y_{i3}) are given in (2.2). Again these obstacle avoidance functions are appropriately coupled with tuning parameters to develop the required repulsive potential field functions.

3.2.2 Stationary Obstacles

Let us fix q stationary obstacles within the boundaries of the workspace. We assume that the lth stationary obstacle is circular with center given as (o_{l1}, o_{l2}) and radius rad_l, and defined as

$$O_l := \{(z_1, z_2) \in \mathbb{R}^2 : (z_1 - o_{l1})^2 + (z_2 - o_{l2})^2 \leq rad_l^2\},$$

for $l = 1, 2, \ldots, q$. For its avoidance we will need to construct separate avoidance functions for each m body of A_i. Thus we consider

$$FO_{iml}(\mathbf{x}) \;=\; \frac{1}{2}\left[(x_{im} - o_{l1})^2 + (y_{im} - o_{l2})^2 - (r_m + rad_l)^2\right], \tag{3.5}$$

for $m = 1, 2, 3$, $l = 1, 2, \ldots, q$ and $i = 1, 2, \ldots, n$. The functions $FO_{i1l}(\mathbf{x})$, $FO_{i2l}(\mathbf{x})$ and $FO_{3li}(\mathbf{x})$ are the measures of the distance between the lth stationary obstacle and the platform, Link 1, and Link 2, respectively.

3.2.3 Antitargets: Targets as Obstacles

In the interest of autonomy, it necessitates that we treat the target of a 2MM as a fixed obstacle for the remaining 2MMs traversing the workspace. Therefore for the mth body of A_i to avoid the target of A_j, we utilize the obstacle avoidance function

$$TO_{imj}(\mathbf{x}) \;=\; \frac{1}{2}\left[(x_{im} - p_{j1})^2 + (y_{im} - p_{j2})^2 - (r_m + rt_j)^2\right], \tag{3.6}$$

for $m = 1, 2, 3$ and $i, j = 1, \ldots, n,\ j \neq i$. we note that function $TO_{imj}(\mathbf{x})$ is positive over the domain $\left\{\mathbf{x} \in \mathbb{R}^{9\times n} : (x_{im} - p_{j1})^2 + (y_{im} - p_{j2})^2 > (r_m + rt_j)^2\right\}$.

3.2.4 Moving Obstacles

Each solid body of an articulated 2MM has to be treated as a moving obstacle for all the other 2MMs in the workspace. Therefore, for each mth body of A_i to avoid the uth moving body of A_j, we shall use the avoidance function

$$MO_{imju}(\mathbf{x}) \;=\; \frac{1}{2}\left[(x_{im} - x_{ju})^2 + (y_{im} - y_{ju})^2 - (r_m + r_u)^2\right], \tag{3.7}$$

for $m, u = 1, 2, 3$ and $i, j = 1, \ldots, n,\ j \neq i$. We further note that $MO_{imju}(\mathbf{x})$ is positive over the domain $\left\{\mathbf{x} \in \mathbb{R}^{9\times n} : (x_{im} - x_{ju})^2 + (y_{im} - y_{ju})^2 > (r_m + r_u)^2\right\}$.

3.3 Dynamic Constraints

Mechanical singularities and bounds on velocities are treated as dynamic constraints. In practice, bending angles of the links are limited due to the mechanical singularities, while the velocities of the links and the wheeled platform are restricted due to safety reasons. In accordance with the Lyapunov-based control scheme, each dynamic constraint will be treated as an *artificial obstacle* and appropriate obstacle avoidance function will be designed for its avoidance.

3.3.1 Mechanical Singularities

(i) Singular configurations arise when $\theta_{i3} = 0$, $\theta_{i3} = \pi$ or $\theta_{i3} = -\pi$. Subsequently, the condition placed on θ_{i3} is $0 < |\theta_{i3}| < \pi$ for $\theta_{i3} \in (-\pi, 0) \cup (0, \pi)$, which implies that Link 2 can neither be fully stretched nor be folded back [24];

(ii) The angle between Link 1 and the platform is bounded by $-\pi/2 < \theta_{i2} < \pi/2$. Simply worded, Link 1 of the ith 2MM can only freely rotate within $\left(-\frac{\pi}{2}, \frac{\pi}{2}\right)$.

Based on these constraints, the following artificial obstacles can be constructed:

$$AO_{i1} = \{\theta_{i3} \in \mathbb{R} : \theta_{i3} = 0, \theta_{i3} = \pi \text{ or } \theta_{i3} = -\pi\};$$
$$AO_{i2} = \{\theta_{i2} \in \mathbb{R} : \theta_{i2} \leq -\frac{\pi}{2} \text{ or } \theta_{i2} \geq \frac{\pi}{2}\}.$$

For avoidance, the following obstacle avoidance functions will be included:

$$S_{i1}(\mathbf{x}) = |\theta_{i3}|; \;\; S_{i2}(\mathbf{x}) = \pi - |\theta_{i3}|; \;\; S_{i3}(\mathbf{x}) = \frac{1}{2}\left(\frac{\pi}{2} - \theta_{i2}\right)\left(\frac{\pi}{2} + \theta_{i2}\right). \tag{3.8a-c}$$

These positive functions would guarantee a strict observation of the mechanical singularities when encoded appropriately into specific repulsive potential field functions, which in turn, would be summed to the Lyapunov function.

3.3.2 Modulus Bound on Velocities

From a practical viewpoint, the translational and rotational velocities of the 2MMs are limited, so we include constraints:

(i) $|v_i| < v_{\max}$, where $v_{\max}$ is the *maximal achievable speed*;

(ii) $|\omega_{i1}| < \frac{v_{\max}}{|\rho_{\min}|}$, where $\rho_{\min} = \frac{\ell_0}{\tan(\phi_{\max})}$. This condition arises due to the boundness of the steering angle, ϕ_i. That is $|\phi_i| \leq \phi_{\max}$, where $\phi_{\max}$ is *maximal steering angle*;

(iii) $|\omega_{i2}| < \omega_{2\,\max}$ and $|\omega_{i3}| < \omega_{3\,\max}$, where $\omega_{2\,\max}$ and $\omega_{3\,\max}$ are the *maximal rotational velocities* of Link 1 and Link 2, respectively.

To ensure that A_i operates within these constraints the following artificial obstacles can be constructed:

$$AO_{i3} = \{\upsilon_i \in \mathbb{R} : \upsilon_i \leq -\upsilon_{\max} \text{ or } \upsilon_i \geq \upsilon_{\max}\},$$
$$AO_{i4} = \{\omega_i \in \mathbb{R} : \omega_i \leq -\upsilon_{\max}/|\rho_{\min}| \text{ or } \omega_i \geq \upsilon_{\max}/|\rho_{\min}|\}.$$

The following obstacle avoidance functions will be designed for A_i for the avoidance of these artificial obstacles:

$$U_{i1}(\mathbf{x}) = \frac{1}{2}\left(v_{\max}^2 - v_i^2\right) , \qquad U_{i2}(\mathbf{x}) = \frac{1}{2}\left(\frac{v_{\max}^2}{\rho_{\min}^2} - \omega_{i1}^2\right), \tag{3.9a-b}$$

$$U_{i3}(\mathbf{x}) = \frac{1}{2}\left(\omega_{2\max}^2 - \omega_{i2}^2\right), \qquad U_{i4}(\mathbf{x}) = \frac{1}{2}\left(\omega_{3\max}^2 - \omega_{i3}^2\right), \tag{3.9c-d}$$

for $i = 1, 2, \ldots, n$. These positive functions would guarantee the adherence to limitations placed upon the steering angle and the velocities when encoded appropriately into the repulsive potential field functions, which in turn, would be summed to the Lyapunov function.

3.4 Auxiliary Function

To guarantee the convergence of a 2MM to its target and to ensure that the nonlinear controllers vanish at this target, we design a new auxiliary function that would be multiplied to each of the repulsive potential field function mentioned above. This is in line with the work in [16, 24]. A reliable choice of the auxiliary function can be :

$$F_i(\mathbf{x}) \;=\; \frac{1}{2}\left[(x_i - p_{i1})^2 + (y_i - p_{i2})^2 + \sum_{j=1}^{3} \rho_{ij}(\theta_{ij} - p_{ij+2})^2\right]. \tag{3.10}$$

3.5 Lyapunov-based Control Scheme

Utilizing the Lyapunov-based control scheme we design the nonlinear control laws for our kinodynamic system (2.1). In parallel, the control scheme utilizes Lyapunov's Second Method to provide a mathematical proof of stability of (2.1). Lyapunov's Second Method, established in 1892, provides one of the most powerful means of analyzing nonlinear systems because of the qualitative information it is able to provide on the system.

We begin the process of stability analysis with the following theorem:

Theorem 3.1 *Consider multiple 2-link mobile manipulators, the motions of which are governed by ODEs described by system (2.1). The objective is to, amongst considering other integrated subtasks, control the motions of these multi-robots within a constrained environment and attain prescribed final postures. The subtasks include; observing workspace restrictions, generating practical parking maneuvers, obtaining final orientations, convergence to predefined targets, and consideration of kinodynamic constraints. The Lyapunov-based control scheme generates the following continuous time-invariant control laws for* A_i

as well as guarantees stability of system (2.1) per se:

$$\left.\begin{aligned}
u_{i1} =& -\left[\delta_{i1} v_i + (f_{i1} + f_{i3} + f_{i5} + f_{i7}) \cos\theta_{i1}\right. \\
&\left. + (f_{i2} + f_{i4} + f_{i6} + f_{i8}) \sin\theta_{i1}\right] / h_{i1}, \\
u_{i2} =& -\left[\delta_{i2}\omega_{i1} - \left(f_{i1} + \frac{1}{2} f_{i3} + f_{i5} + f_{i7}\right) \ell_0 \sin\theta_{i1}\right. \\
&+ \left(f_{i2} + \frac{1}{2} f_{i4} + f_{i6} + f_{i8}\right) \ell_0 \cos\theta_{i1} \\
&- \left(f_{i1} + \frac{1}{2} f_{i5} + f_{i7}\right) \ell_1 \sin\theta_{iQ} + \left(f_{i2} + \frac{1}{2} f_{i6} + f_{i8}\right) \ell_1 \cos\theta_{iQ} \\
&\left. - \left(f_{i1} + \frac{1}{2} f_{i7}\right) \ell_2 \sin\theta_{iT} + \left(f_{i2} + \frac{1}{2} f_{i8}\right) \ell_2 \cos\theta_{iT} + g_{i1}\right] / h_{i2}, \\
u_{i3} =& -\left[\delta_{i3}\omega_{i2} - \left(f_{i1} + \frac{1}{2} f_{i5} + f_{i7}\right) \ell_1 \sin\theta_{iQ}\right. \\
&+ \left(f_{i2} + \frac{1}{2} f_{i6} + f_{i8}\right) \ell_1 \cos\theta_{iQ} - \left(f_{i1} + \frac{1}{2} f_{i7}\right) \ell_2 \sin\theta_{iT} \\
&\left. + \left(f_{i2} + \frac{1}{2} f_{i8}\right) \ell_2 \cos\theta_{iT} + g_{i2}\right] / h_{i3}, \\
u_{i4} =& -\left[\delta_{i4}\omega_{i3} - \left(f_{i1} + \frac{1}{2} f_{i7}\right) \ell_2 \sin\theta_{iT}\right. \\
&\left. + \left(f_{i2} + \frac{1}{2} f_{i8}\right) \ell_2 \cos\theta_{iT} + g_{i3}\right] / h_{i4},
\end{aligned}\right\} \tag{3.11}$$

where $\theta_{iQ} = \theta_{i1} + \theta_{i2}$, $\theta_{iT} = \theta_{i1} + \theta_{i2} + \theta_{i3}$, $\omega_{iQ} = \omega_{i1} + \omega_{i2}$, $\omega_{iT} = \omega_{i1} + \omega_{i2} + \omega_{i3}$ *and* $\delta_{iv} > 0$ *for* $v = 1, \ldots, 4$ *and* $i = 1, \ldots, n$ *are the convergence parameters.*

Proof: Combining the new auxiliary function, the potential field functions created from the attractive and obstacle avoidance functions from the previous sections, and introducing *tuning parameters* (or control parameters), $\alpha_{is} > 0$, $\xi_{ip} > 0$, $\gamma_{iml} > 0$, $\varphi_{imk} > 0$, $\beta_{ir} > 0$, $\zeta_{imj} > 0$ and $\psi_{imju} > 0$, for $\{i, j, m, s, p, l, k, u, r\} \in \mathbb{N}$, we define a Lyapunov function candidate $L : \mathbb{R}^n \to \mathbb{R}$ for system (2.1) as

$$\begin{aligned}
L(\mathbf{x}) \;=\; & \sum_{i=1}^{n} \left\{ V_i(\mathbf{x}) + F_i(\mathbf{x}) \left[\sum_{s=1}^{8} \frac{\alpha_{is}}{W_{is}(\mathbf{x})} + \sum_{m=1}^{3} \left(\sum_{l=1}^{q} \frac{\gamma_{iml}}{FO_{iml}(\mathbf{x})} \right.\right.\right. \\
& \left. + \sum_{k=1}^{2n} \frac{\varphi_{imk}}{LS_{imk}(\mathbf{x})} + \sum_{\substack{j=1 \\ j \neq i}}^{n} \left[\frac{\zeta_{imj}}{TO_{imj}(\mathbf{x})} + \sum_{u=1}^{3} \frac{\psi_{imju}}{MO_{imju}(\mathbf{x})} \right] \right) \\
& \left. \left. + \sum_{p=1}^{3} \frac{\xi_{ip}}{S_{ip}(\mathbf{x})} + \sum_{r=1}^{4} \frac{\beta_{ir}}{U_{ir}(\mathbf{x})} \right] \right\}.
\end{aligned} \tag{3.12}$$

Assumption: A fixed point $\mathbf{x}_i^* = (p_{i1}, p_{i2}, p_{i3}, p_{i4}, p_{i5}, 0, 0, 0, 0) \in \mathbb{R}^9$ is an equilibrium point for the end effector of A_i, then we have $\mathbf{x}_e = (\mathbf{x}_1^*, \mathbf{x}_2^*, \ldots, \mathbf{x}_n^*) \in D(L)$ as, at least, an equilibrium state for the kinodynamic system (2.1).

Remark: *If we let* $\frac{dL}{dt} = f(\mathbf{x})$ *then* $f(\mathbf{x}_e) \equiv 0$ *making* $\mathbf{x}_e$ *a feasible equilibrium point, at least, in a small neighborhood of the target configuration.*

In addition, one can easily verify the following:

1. L is continuous and positive on the domain $\mathbb{D}$ given as

$$\begin{aligned} D(L) \;=\; & \{\mathbf{x} \in \mathbb{R}^{9\times n} : W_{is}(\mathbf{x}) > 0, s = 1, \ldots, 8;\ S_{ip}(\mathbf{x}) > 0, p = 1, \ldots, 3; \\ & (FO_{iml}(\mathbf{x}) > 0, l = 1, \ldots, q;\ LS_{imk}(\mathbf{x}) > 0, k = 1, \ldots, 2n, m = 1, 2, 3), \\ & U_{ir}(\mathbf{x}) > 0, r = 1, \ldots, 4;\ (TO_{imj}(\mathbf{x}) > 0, \\ & MO_{imju}(\mathbf{x}) > 0, m, u = 1, 2, 3, j \neq i, j = 1, \ldots, n), \text{for } i = 1, \ldots, n\}. \end{aligned}$$

2. $L(\mathbf{x}_e) = 0,\ \mathbf{x}_e \in \mathbb{D}$.

3. $L(\mathbf{x}) > 0\ \ \forall\, \mathbf{x} \in \mathbb{D}, \mathbf{x} \neq \mathbf{x}_e$.

Now let us consider the time derivative of the Lyapunov function candidate along a particular trajectory of system (2.1):

$$\begin{aligned} \dot{L}(\mathbf{x}) \;=\; & \sum_{i=1}^{n} \{[(f_{i1} + f_{i3} + f_{i5} + f_{i7}) \cos\theta_{i1} + (f_{i2} + f_{i4} + f_{i6} + f_{i8}) \sin\theta_{i1} + h_{i1}u_{i1}]\, v_i \\ & + \left[-\left(f_{i1} + \frac{1}{2}f_{i3} + f_{i5} + f_{i7}\right) \ell_0 \sin\theta_{i1} + \left(f_{i2} + \frac{1}{2}f_{i4} + f_{i6} + f_{i8}\right) \ell_0 \cos\theta_{i1} \right. \\ & \quad - \left(f_{i1} + \frac{1}{2}f_{i5} + f_{i7}\right) \ell_1 \sin\theta_{iQ} + \left(f_{i2} + \frac{1}{2}f_{i6} + f_{i8}\right) \ell_1 \cos\theta_{iQ} \\ & \quad \left. - \left(f_{i1} + \frac{1}{2}f_{i7}\right) \ell_2 \sin\theta_{iT} + \left(f_{i2} + \frac{1}{2}f_{i8}\right) \ell_2 \cos\theta_{iT} + g_{i1} + h_{i2}u_{i2} \right] \omega_{i1} \\ & + \left[-\left(f_{i1} + \frac{1}{2}f_{i5} + f_{i7}\right) \ell_1 \sin\theta_{iQ} + \left(f_{i2} + \frac{1}{2}f_{i6} + f_{i8}\right) \ell_1 \cos\theta_{iQ} \right. \\ & \quad \left. - \left(f_{i1} + \frac{1}{2}f_{i7}\right) \ell_2 \sin\theta_{iT} + \left(f_{i2} + \frac{1}{2}f_{i8}\right) \ell_2 \cos\theta_{iT} + g_{i2} + h_{i3}u_{i3} \right] \omega_{i2} \\ & + \left[-\left(f_{i1} + \frac{1}{2}f_{i7}\right) \ell_2 \sin\theta_{iT} + \left(f_{i2} + \frac{1}{2}f_{i8}\right) \ell_2 \cos\theta_{iT} + g_{i3} + h_{i4}u_{i4} \right] \omega_{i3} \Bigg\}, \end{aligned}$$

where the functions f_{i1} to f_{i8}, g_{i1} to g_{i3}, and h_{i1} to h_{i4}, for $i = 1, 2, \ldots, n$ and $v = 1, \ldots, 4$, are defined as (on suppressing $\mathbf{x}$):

$$\begin{aligned} f_{i1} \;=\; & \left\{ 1 + \sum_{s=1}^{8} \frac{\alpha_{is}}{W_{is}} + \sum_{m=1}^{3} \left[\sum_{l=1}^{q} \frac{\gamma_{iml}}{FO_{iml}} + \sum_{k=1}^{2n} \frac{\varphi_{imk}}{LS_{imk}} + \sum_{\substack{j=1 \\ j\neq i}}^{n} \left(\frac{\zeta_{imj}}{TO_{imj}} + \sum_{u=1}^{3} \frac{\psi_{imju}}{MO_{imju}} \right) \right] \right. \\ & \left. + \sum_{p=1}^{3} \frac{\xi_{ip}}{S_{ip}} + \sum_{r=1}^{4} \frac{\beta_{ir}}{U_{ir}} \right\} (x_i - p_{i1}), \end{aligned}$$

$$
\begin{aligned}
f_{i2} &= \left\{ 1 + \sum_{s=1}^{8} \frac{\alpha_{is}}{W_{is}} + \sum_{m=1}^{3} \left[\sum_{l=1}^{q} \frac{\gamma_{iml}}{FO_{iml}} + \sum_{k=1}^{2n} \frac{\varphi_{imk}}{LS_{imk}} + \sum_{\substack{j=1 \\ j\neq i}}^{n} \left(\frac{\zeta_{imj}}{TO_{imj}} + \sum_{u=1}^{3} \frac{\psi_{imju}}{MO_{imju}} \right) \right] \right. \\
&\quad \left. + \sum_{p=1}^{3} \frac{\xi_{ip}}{S_{ip}} + \sum_{r=1}^{4} \frac{\beta_{ir}}{U_{ir}} \right\} (y_i - p_{i2}), \\
f_{i3} &= -F_i \left\{ \frac{\alpha_{i1}}{W_{i1}^2} - \frac{\alpha_{i3}}{W_{i3}^2} + \sum_{l=1}^{q} \frac{\gamma_{i1l}}{FO_{i1l}^2} (x_{i1} - o_{l1}) \right. \\
&\quad \left. + \sum_{k=1}^{2} \frac{\psi_{i1k}}{LS_{i1k}^2} \left[(1 - (a_{k2} - a_{k1}) q_{k1}) (x_{i1} - c_{i1k}) - (b_{k2} - b_{k1}) q_{k1} (y_{i1} - d_{i1k}) \right] \right\} \\
&\quad - \sum_{\substack{j=1 \\ j\neq i}}^{n} \left[\frac{\zeta_{i1j}}{TO_{i1j}^2} F_i (x_{i1} - p_{j1}) + \sum_{u=1}^{3} \left(\frac{\psi_{i1ju}}{MO_{i1ju}^2} F_i + \frac{\psi_{jui1}}{MO_{jui1}^2} F_j \right) (x_{i1} - x_{ju}) \right], \\
f_{i4} &= -F_i \left\{ \frac{\alpha_{i2}}{W_{i2}^2} - \frac{\alpha_{i4}}{W_{i4}^2} + \sum_{l=1}^{q} \frac{\gamma_{i1l}}{FO_{i1l}^2} (y_{i1} - o_{l2}) \right. \\
&\quad \left. + \sum_{k=1}^{2n} \frac{\psi_{i1k}}{LS_{i1k}^2} \left[(1 - (b_{k2} - b_{k1}) q_{k2}) (y_{i1} - d_{i1k}) - (a_{k2} - a_{k1}) q_{k2} (x_{i1} - c_{i1k}) \right] \right\} \\
&\quad - \sum_{\substack{j=1 \\ j\neq i}}^{n} \left[\frac{\zeta_{i1j}}{TO_{i1j}^2} F_i (y_{i1} - p_{j2}) + \sum_{u=1}^{3} \left(\frac{\psi_{i1ju}}{MO_{i1ju}^2} F_i + \frac{\psi_{jui1}}{MO_{jui1}^2} F_j \right) (y_{i1} - y_{ju}) \right], \\
f_{i5} &= -F_i \left\{ \sum_{l=1}^{q} \frac{\gamma_{i2l}}{FO_{i2l}^2} (x_{i2} - o_{l1}) \right. \\
&\quad \left. + \sum_{k=1}^{2n} \frac{\psi_{i2k}}{LS_{i2k}^2} \left[(1 - (a_{k2} - a_{k1}) q_{k1}) (x_{i2} - c_{i2k}) - (b_{k2} - b_{k1}) q_{k1} (y_{i2} - d_{i2k}) \right] \right\} \\
&\quad - \sum_{\substack{j=1 \\ j\neq i}}^{n} \left[\frac{\zeta_{i2j}}{TO_{i2j}^2} F_i (x_{i2} - p_{j1}) + \sum_{u=1}^{3} \left(\frac{\psi_{i2ju}}{MO_{i2ju}^2} F_i + \frac{\psi_{jui2}}{MO_{jui2}^2} F_j \right) (x_{i2} - x_{ju}) \right], \\
f_{i6} &= -F_i \left\{ \sum_{l=1}^{q} \frac{\gamma_{i2l}}{FO_{i2l}^2} (y_{i2} - o_{l2}) \right. \\
&\quad \left. + \sum_{k=1}^{2n} \frac{\psi_{i2k}}{LS_{i2k}^2} \left[(1 - (b_{k2} - b_{k1}) q_{k2}) (y_{i2} - d_{i2k}) - (a_{k2} - a_{k1}) q_{k2} (x_{i2} - c_{i2k}) \right] \right\} \\
&\quad - \sum_{\substack{j=1 \\ j\neq i}}^{n} \left[\frac{\zeta_{i2j}}{TO_{i2j}^2} F_i (y_{i2} - p_{j2}) + \sum_{u=1}^{3} \left(\frac{\psi_{i2ju}}{MO_{i2ju}^2} F_i + \frac{\psi_{jui2}}{MO_{jui2}^2} F_j \right) (y_{i2} - y_{ju}) \right],
\end{aligned}
$$

$$
\begin{aligned}
f_{i7} &= -F_i \Bigg\{ \frac{\alpha_{i5}}{W_{i5}^2} - \frac{\alpha_{i7}}{W_{i7}^2} + \sum_{l=1}^{q} \frac{\gamma_{i3l}}{FO_{i3l}^2} \left(x_{i3} - o_{l1}\right) \\
&\quad + \sum_{k=1}^{2n} \frac{\psi_{i3k}}{LS_{i3k}^2} \left[\left(1 - (a_{k2} - a_{k1}) q_{k1}\right) \left(x_{i3} - c_{i3k}\right) - (b_{k2} - b_{k1}) q_{k1} \left(y_{i3} - d_{i3k}\right) \right] \Bigg\} \\
&\quad - \sum_{\substack{j=1 \\ j \neq i}}^{n} \left[\frac{\zeta_{i3j}}{TO_{i3j}^2} F_i \left(x_{i3} - p_{j1}\right) + \sum_{u=1}^{3} \left(\frac{\psi_{i3ju}}{MO_{i3ju}^2} F_i + \frac{\psi_{jui3}}{MO_{jui3}^2} F_j \right) \left(x_{i3} - x_{ju}\right) \right], \\
f_{i8} &= -F_i \Bigg\{ \frac{\alpha_{i6}}{W_{i6}^2} - \frac{\alpha_{i8}}{W_{i8}^2} + \sum_{l=1}^{q} \frac{\gamma_{i3l}}{FO_{i3l}^2} \left(y_{i3} - o_{l2}\right) \\
&\quad + \sum_{k=1}^{2n} \frac{\psi_{i3k}}{LS_{i3k}^2} \left[\left(1 - (b_{k2} - b_{k1}) q_{k2}\right) \left(y_{i3} - d_{i3k}\right) - (a_{k2} - a_{k1}) q_{k2} \left(x_{i3} - c_{i3k}\right) \right] \Bigg\} \\
&\quad - \sum_{\substack{j=1 \\ j \neq i}}^{n} \left[\frac{\zeta_{i3j}}{TO_{i3j}^2} F_i \left(y_{i3} - p_{j2}\right) + \sum_{u=1}^{3} \left(\frac{\psi_{i3ju}}{MO_{i3ju}^2} F_i + \frac{\psi_{jui3}}{MO_{jui3}^2} F_j \right) \left(y_{i3} - y_{ju}\right) \right], \\
g_{i1} &= \Bigg\{ \sum_{s=1}^{8} \frac{\alpha_{is}}{W_{is}} + \sum_{m=1}^{3} \left[\sum_{l=1}^{q} \frac{\gamma_{iml}}{FO_{iml}} + \sum_{k=1}^{2n} \frac{\varphi_{imk}}{LS_{imk}} + \sum_{\substack{j=1 \\ j \neq i}}^{n} \left(\frac{\zeta_{imj}}{TO_{imj}} + \sum_{u=1}^{3} \frac{\psi_{imju}}{MO_{imju}} \right) \right] \\
&\quad + \sum_{p=1}^{3} \frac{\xi_{ip}}{S_{ip}} + \sum_{r=1}^{4} \frac{\beta_{ir}}{U_{ir}} \Bigg\} \rho_{i1} (\theta_{i1} - p_{i3}) \, , \\
g_{i2} &= \Bigg\{ \sum_{s=1}^{8} \frac{\alpha_{is}}{W_{is}} + \sum_{m=1}^{3} \left[\sum_{l=1}^{q} \frac{\gamma_{iml}}{FO_{iml}} + \sum_{k=1}^{2n} \frac{\varphi_{imk}}{LS_{imk}} + \sum_{\substack{j=1 \\ j \neq i}}^{n} \left(\frac{\zeta_{imj}}{TO_{imj}} + \sum_{u=1}^{3} \frac{\psi_{imju}}{MO_{imju}} \right) \right] \\
&\quad + \sum_{p=1}^{3} \frac{\xi_{ip}}{S_{ip}} + \sum_{r=1}^{4} \frac{\beta_{ir}}{U_{ir}} \Bigg\} \rho_{i2} (\theta_{i2} - p_{i4}) + F_i \frac{\xi_{i3}}{S_{i3}^2} \theta_{i2}, \\
g_{i3} &= \Bigg\{ \sum_{s=1}^{8} \frac{\alpha_{is}}{W_{is}} + \sum_{m=1}^{3} \left[\sum_{l=1}^{q} \frac{\gamma_{iml}}{FO_{iml}} + \sum_{k=1}^{2n} \frac{\varphi_{imk}}{LS_{imk}} + \sum_{\substack{j=1 \\ j \neq i}}^{n} \left(\frac{\zeta_{imj}}{TO_{imj}} + \sum_{u=1}^{3} \frac{\psi_{imju}}{MO_{imju}} \right) \right] \\
&\quad + \sum_{p=1}^{3} \frac{\xi_{ip}}{S_{ip}} + \sum_{r=1}^{4} \frac{\beta_{ir}}{U_{ir}} \Bigg\} \rho_{i3} (\theta_{i3} - p_{i5}) - F_i \left(\frac{\xi_{i1}}{S_{i1}^2} - \frac{\xi_{i2}}{S_{i2}^2} \right) \frac{|\theta_{i3}|}{\theta_{i3}}, \\
h_{iv} &= 1 + \frac{\beta_{iv}}{U_{iv}^2} F_i.
\end{aligned}
$$

Substituting the controllers given in (3.11) and the governing ODEs for system (2.1) we obtain a semi-negative definite function

$$
\dot{L}(\mathbf{x}) = -\sum_{i=1}^{n} \left(\delta_{i1} v_i^2 + \delta_{i2} \omega_{i1}^2 + \delta_{i3} \omega_{i2}^2 + \delta_{i4} \omega_{i3}^2 \right) \leq 0 \, .
$$

We have thus provided a working proof of the fact that $\frac{d}{dt}[L(\mathbf{x})] \leq 0 \ \ \forall\, \mathbf{x} \in \mathbb{D}$. Finally, the first partials of $L(\mathbf{x})$ is C^1 which makes up the fifth and final prerequisite required of a Lyapunov function.

When $L(\mathbf{x})$ successfully meets the five prerequisites discussed above, it is classified as a Lyapunov function for system (2.1) and $\mathbf{x}_e$ is at least a stable equilibrium point in the sense of Lyapunov. In our case, this practical limitation is well within the Lyapunov framework and there is no contradiction with Brockett's result because we have proven only stability, and not asymptotic stability. Stability means that any solution of (2.1) starting close to $\mathbf{x}_e$ remains near it at all times.

3.6 Scenario 1

The first scenario captures a possible traffic situation to illustrate the effectiveness of the control laws proposed in the paper. We have fabricated a situation wherein two 2MMs have to maneuver from an initial to a final state and park correctly inside the prescribed diagonal-structured parking bay, whilst avoiding obstacles in their path. The corresponding states, workspace and parking bay restrictions, singularities and other essentials of the simulation are tabulated below (see Tables 1 and 2).

Table 1: Initial and Final States

	2MM 1	2MM 2
Rect. Position : (x_{i1}, y_{i1})	$(5,\ 3)\ m$	$(5,\ 25)\ m$
Angular Position : $(\theta_{i1}, \theta_{i2}, \theta_{i3})$	$(0, \pi/3, -2\pi/3)\ rad$	$(0, \pi/3, -2\pi/3)\ rad$
Translational Velocity : (v_i)	$5\ m/s$	$5\ m/s$
Rotational Vel. : $(\omega_{i1}, \omega_{i2}, \omega_{i3})$	$(0.3, 0.05, 0.05)\ rad/s$	$(0.3, 0.05, 0.05)\ rad/s$
Final Position: (p_{i1}, p_{i2})	$((26.4, 26.4)\ m$	$(26.3, 2)\ m$
Final Orientation : (p_{i3}, p_{i4}, p_{i5})	$(\pi/4, \pi/4, -\pi/2)\ rad$	$(-\pi/3, \pi/4, -\pi/2)\ rad$

Table 2: Values of Constraints and Parameters

	Constraints and Parameters
Clearance Parameters	$\epsilon_1 = 0.2\ m$, $\epsilon_2 = 0.1\ m$, $\epsilon_3 = 0.3\ m$
Robot Dimensions	$\ell_0 = 2\ m$, $b_0 = 1\ m$, $\ell_1 = \ell_2 = 1.2\ m$
Obstacle Center, Radius	$(o_{11}, o_{12}) = (12\ m, 15\ m)$, $rad_1 = 2\ m$
Max. Steering Angle	$\phi_{\max} = 7\pi/18\ rad$
Max. Velocities	$v_{\max} = 10\ m/s$, $\omega_{2\max} = \omega_{3\max} = 1\ rad/s$
Top, Right Boundaries	$\eta_1 = \eta_2 = 28\ m$
Control Parameters	$\alpha_{1s} = 0.01$, $s = 1, \ldots, 8$, $\gamma_{m1i} = 0.5$, $m = 1, 2, 3$;
	$\zeta_{m1i} = 0.1$, $\zeta_{m2i} = 1$, $\xi_{ip} = 0.5$, $p = 1, 2, 3$;
	$\beta_{ir} = 0.1$, $r = 1, \ldots, 4$;
	$\psi_{imj} = 1$, $\varphi_{imju} = 0.5$, $m, u = 1, 2, 3$, $i, j = 1, 2$, $j \neq i$
Angle-gain parameter	$\rho_{ij} = 1$, $i = 1, 2 \ \ j = 1, 2, 3$
Convergence Parameters	$\delta_{i1} = \delta_{i2} = \delta_{i3} = \delta_{i4} = 15$
Parking Bays	can be obtained from Fig. 2

Figure 2 shows feasible trajectories from initial to the final states. In the final phase, the wheeled platforms and the links of each 2MM achieved the prescribed final orientations.

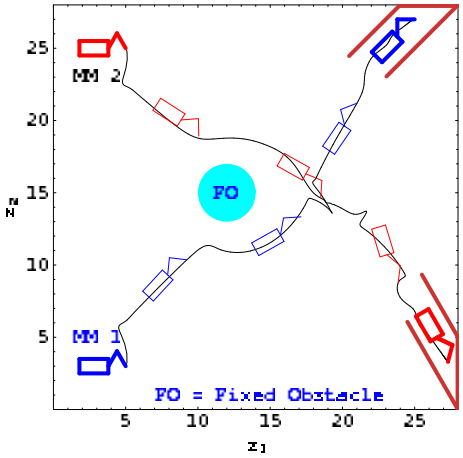

Figure 2: The resulting trajectories of the 2MMs in a traffic scenario.

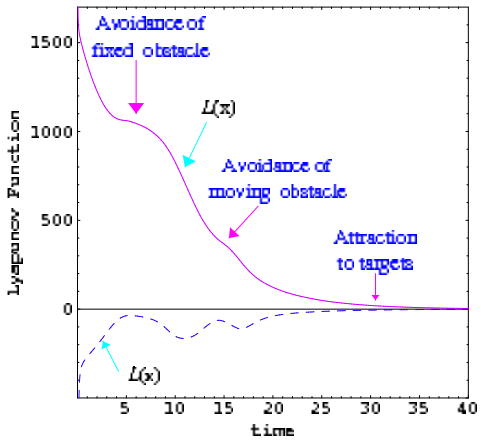

Figure 3: Lyapunov function $L(\mathbf{x})$ and its derivative $\dot{L}(\mathbf{x})$.

Figure 3 shows the evolution of the Lyapunov function and its time derivative along the system trajectory. One can clearly see the decreasing nature of the scalar function. To further illustrate the convergent property of the control laws, we have generated the graphs of the acceleration components of 2MM 1 (shown in Figures 4, and 5).

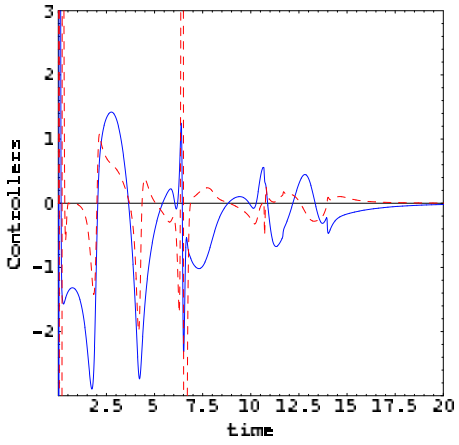

Figure 4: The translational u_{11} (solid line) and rotational u_{12} accelerations of the platform.

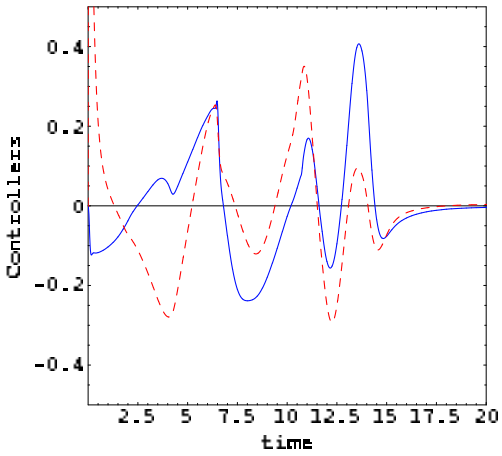

Figure 5: The rotational accelerations u_{13} of Link 1 (solid line) and u_{14} of Link 2.

3.7 Scenario 2

In this scenario, we have considered four 2MMs in a variant traffic "roundabout" situation each travelling around a circular island and peeling off at the relevant street in order to reach the prescribed final posture inside of the designated parking bay. The 2MMs will have to avoid all fixed and moving obstacles intercepting their paths. Tables 3 and 4 show the essentials for the simulation. However, we have omitted those details (including the units) that have not changed from scenario 1.

Table 3: Initial and Final States

	2MM 1	2MM 2	2MM 3	2MM 4
Rectangular Position (x_i, y_i)	$(5, 14)$	$(14, 23)$	$(23, 14)$	$(14, 5)$
Angular Positions $(\theta_{i1}, \theta_{i2}, \theta_{i3})$	$(0, \frac{\pi}{3}, -\frac{2\pi}{3})$	$(-\frac{\pi}{2}, \frac{\pi}{3}, -\frac{2\pi}{3})$	$(\pi, \frac{\pi}{3}, -\frac{2\pi}{3})$	$(\frac{\pi}{2}, \frac{\pi}{3}, -\frac{2\pi}{3})$
Translational Vel.	$v_1 = 3$	$v_2 = 3$	$v_3 = 3$	$v_4 = 3$
Rotational Vel. $(\omega_{i1}, \omega_{i2}, \omega_{i3})$	$(0.3, 0.05, 0.05)$	$(0.3, 0.05, 0.05)$	$(0.3, 0.05, 0.05)$	$(0.3, 0.05, 0.05)$
Final Position (p_{i1}, p_{i2})	$(27, 14)$	$(14, 1)$	$(1, 14)$	$(14, 27)$
Final Orientations (p_{i3}, p_{i4}, p_{i5})	$(0, \frac{\pi}{4}, -\frac{\pi}{2})$	$(-\frac{\pi}{2}, \frac{\pi}{4}, -\frac{\pi}{2})$	$(\pi, \frac{\pi}{4}, -\frac{\pi}{2})$	$(\frac{\pi}{2}, \frac{\pi}{4}, -\frac{\pi}{2})$

Table 4: Values of Constraints and Parameters

	Constraints and Parameters
Obstacle Center, Radius	$(o_{11}, o_{12}) = (14\ m, 14\ m)$, $rad_1 = 2\ m$
Control Parameters	$\alpha_{1s} = 0.01$, $s = 1, \ldots, 8$, $\gamma_{m1i} = 0.5$, $m = 1, 2, 3$;
	$\zeta_{m1i} = 0.2$, $\zeta_{m2i} = 1.2$, $\xi_{ip} = 0.5$, $p = 1, 2, 3$;
	$\beta_{ir} = 0.1$, $r = 1, \ldots, 4$;
	$\psi_{imj} = 1$, $\varphi_{imju} = 0.5$, $m, u = 1, 2, 3, i, j = 1, \ldots, 4$, $j \neq i$
Convergence Parameters	$\delta_{i1} = \delta_{i2} = \delta_{i3} = \delta_{i4} = 15$
Parking Bays	can be obtained from Fig. 6

Figure 6 shows the paths taken by the four 2MMs. Evolution of the Lyapunov function and its time derivative along the system trajectory follow a trend similar to that of scenario 1.

The efficiency of the control laws were put to test with various other initial configurations. Convergence was observed for all cases, provided the initial configurations did not intersect with the avoidance regions of the obstacles. Otherwise, in each case, there was a clear convergence to the target with θ_{i1}, θ_{i2} and θ_{i3} in a small neighborhood of the prescribed final orientation (see figure 7). Nonetheless, one must admit that better trajectories are achievable via fine tunings of the control and convergence parameters. To illustrate the convergent property of the control laws, we again generate the graphs of the acceleration components of 2MM 1 (see Figures 8 to 9). The corresponding graphs for the other 2MMs show similar convergent properties.

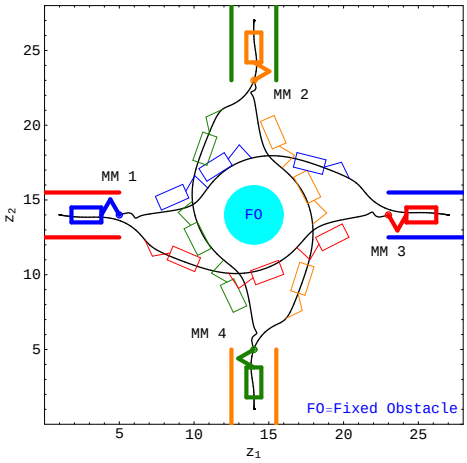

Figure 6: Trajectories of four 2MMs in a constrained environment.

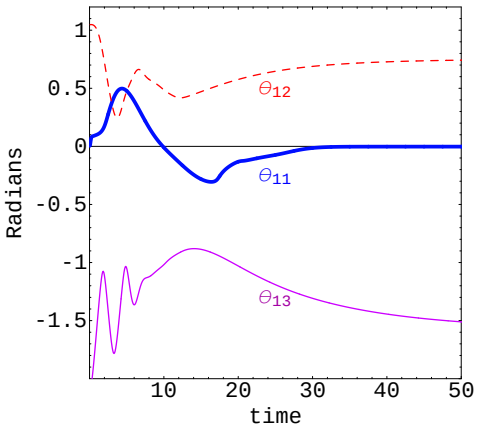

Figure 7: Orientations of platform (bold line), Link 1 and Link 2 (solid line).

4 Conclusion

The authors have presented a set of continuous time-invariant acceleration control laws that successfully tackle the multi-tasking problem of multiple 2-link mobile manipulators posed in this paper. Synthesis of these controllers, for the kinodynamic system, was via the recently developed Lyapunov-based control scheme. The generalized controllers extracted from the control scheme enabled us to obtain collision-free trajectories from initial to desired states within a constrained environment under heavy traffic, whilst satisfying the intimately coupled holonomic and nonholonomic constraints associated with the system. The Lyapunov-based control scheme utilized MDT which further helped guarantee desired parking maneuverabilities and establish feasible prescribed posture of each solid body of the articulated robot in the designated parking bay, a feat accomplished for the first time via continuous controllers. The inclusion of limitations on the translational and rotational velocities of the wheeled platform helped the system mimic the real life mobile manipulators better.

The effectiveness of the proposed control algorithm was demonstrated via a couple of interesting traffic simulations. Although convergence to the prescribed final posture is possible for many initial configurations, further work will be needed to quantify global stability and the region of attraction of the target.

Future work also includes modifying the proposed control algorithm for motion planning in partially known or fully unknown environments, which can include dynamic objects other than the mobile manipulators themselves.

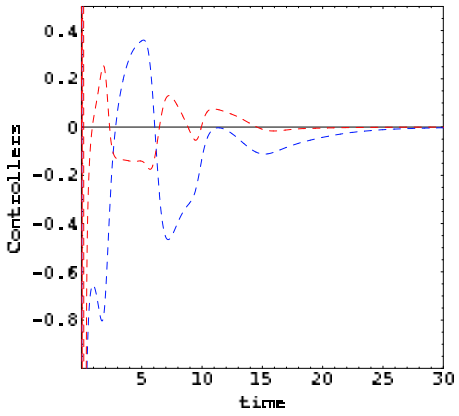

Figure 8: The translational u_{11} (solid line) and rotational u_{12} accelerations of the platform.

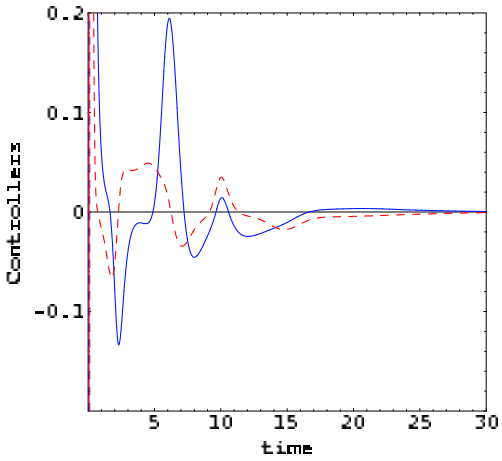

Figure 9: The rotational accelerations u_{13} of Link 1 (solid line) and u_{14} of Link 2.

References

[1] R.W. Brockett. *Differential Geometry Control Theory*, chapter Asymptotic Stability and Feedback Stabilisation, pages 181–191. Springer-Verlag, 1983.

[2] G. Foulon, J.-Y. Fourquet, and M. Renaud. *Experimental Robotics V: Lecture Notes in Control and Information Systems*, chapter Control of a Rover-mounted Manipulator, pages 140–151. Springer, 1998.

[3] G. Foulon, J.-Y. Fourquet, and M. Renaud. Planning point to point paths for nonholonomic mobile manipulators. In *IEEE/RSJ International Conference on Intelligent Robots and Systems*, pages 374–379, Victoria, Canada, October 1998.

[4] G. Foulon, J.-Y. Fourquet, and M. Renaud. Coordinating mobility and manipulation using non-holonomic mobile manipulators. *Control Engineering Practice*, 7:391–399, 1999.

[5] J. L. Fuller. *Introduction, Programming, and Projects.* Prentice Hall, 1998.

[6] Q. Huang, S. Sugano, and K. Tanie. Motion planning for a mobile manipulator considering stability and task constraints. In *Proceedings of the IEEE International Conference on Robotics and Automation*, pages 2192–2198, Leuven, Belgium, May 1998.

[7] V. Kantabutra. Reaching a point with an anchored robot arm in a square. *International Journal of Computational Geometry and Applications*, 7(6):539–549, 1997.

[8] O. Khatib. Real time obstacle avoidance for manipulators and mobile robots. *International Journal of Robotics Research*, 7(1):90–98, 1986.

[9] I. Kolmanovsky and N. McClamroch. Developments in nonholonomic control problems. *IEEE Control Systems Magazine*, 15:20–36, 1995.

[10] A. Matsikis, F. Schulte, F. Broicher, and K. F. Fraiss. A behaviour coordination manager for a mobile manipulator. In *Proceedings of the IEEE/RSJ Int. Conf. on Intelligent Robots and Systems*, pages 174–181, Las Vegas, USA, 2003.

[11] W. Meyer. Moving a planar robot arm. *MAA Notes: The Mathematical Association of America*, (29):180–192, 1993.

[12] E. Papadopoulos and J. Poulakakis. Planning and model-based control for mobile manipulators. In *Procs of the IROS Conference on Intelligent Robots and Systems*, Takamatsu, Japan, 2000.

[13] C. Perrier, P. Dauchez, and F. Pierrot. A global approach for motion generation of non-holonomic mobile manipulator. In *Proceedings of the IEEE International Conference on Robotics and Automation*, pages 2971–2976, Leuven, Belgium, May 1998.

[14] H. Seraji. A unified approach to motion control of mobile manipulators. *International Journal of Robotics Research*, 17(2):107–118, 1998.

[15] B. Sharma. *New Directions in the Applications of the Lyapunov-based Control Scheme to the Findpath Problem.* PhD thesis, University of the South Pacific, Suva, Fiji Islands, July 2008. PhD Dissertation.

[16] B. Sharma and J. Vanualailai. Lyapunov stability of a nonholonomic car-like robotic system. *Nonlinear Studies*, 14(2):143–160, 2007.

[17] B. Sharma, J. Vanualailai, and U. Chand. Flocking of multi-agents in constrained environments. *European Journal of Pure and Applied Mathematics*, 2(3):401–425, 2009.

[18] B. Sharma, J. Vanualailai, and A. Prasad. A lyapunov-based path planning and obstacle avoidance of a two-link manipulator on a wheeled platform. *International Journal of Information Technology*, 14(2):57–75, 2008.

[19] B. Sharma, J. Vanualailai, K. Raghuwaiya, and A. Prasad. New potential field functions for motion planning and posture control of 1-trailer systems. *International Journal of Mathematics and Computer Science*, 3(1):45–71, 2008.

[20] T.G. Sugar and V. Kumar. Control of cooperating mobile manipulators. *IEEE Transactions on Robotics and Automation*, 18(1):94–103, 2002.

[21] H. G. Tanner, S. Loizou, and K. J. Kyriakopoulos. Nonholonomic navigation and control of cooperating mobile manipulators. *IEEE Transactions on Robotics and Automation*, 19(3):53–64, 2003.

[22] J. Vanualailai, J. Ha, and S. Nakagiri. A collision and attraction problem for a vehicle. In *RIMS Symposium*, Kyoto University, Japan, November 2003.

[23] J. Vanualailai and B. Sharma. Moving a robot arm: an interesting application of the Direct Method of Lyapunov. *CUBO: A Mathematical Journal*, 6(3):131–144, 2004.

[24] J. Vanualailai, B. Sharma, and A. Ali. Lyapunov-based kinematic path planning for a 3-link planar robot arm in a structured environment. *Global Journal of Pure and Applied Mathematics*, 3(2):175–190, 2007.

[25] D. Xu, H. Hu, C. A. A. Calderon, and M. Tan. Motion planning for a mobile manipulator with redundant dofs. *International Journal of Information Technology*, 11(11):1–10, 2005.